Article

New Highly Polar Semiconductor Ferroelectrics through *d* Cation-O Vacancy Substitution into PbTiO: A Theoretical Study

Joseph W. Bennett, Ilya Grinberg, and Andrew M. Rappe

J. Am. Chem. Soc., **2008**, 130 (51), 17409-17412 • DOI: 10.1021/ja8052249 • Publication Date (Web): 21 November 2008

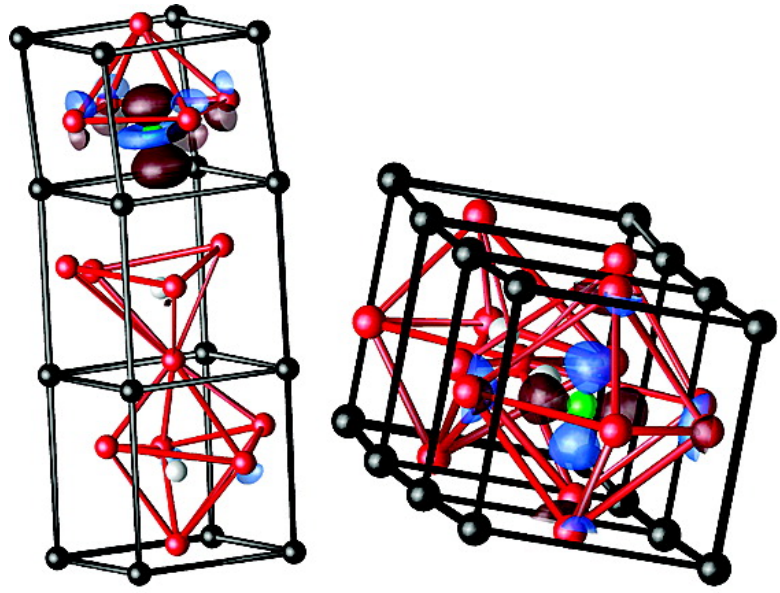

(a) (b)

J|A|C|S
ARTICLES

Published on Web 11/21/2008

New Highly Polar Semiconductor Ferroelectrics through d^8 Cation-O Vacancy Substitution into $PbTiO_3$: A Theoretical Study

Joseph W. Bennett, Ilya Grinberg, and Andrew M. Rappe*

The Makineni Theoretical Laboratories, Department of Chemistry, Philadelphia, Pennsylvania 19104

Received July 7, 2008; E-mail: rappe@sas.upenn.edu

Abstract: We use first-principles density functional theory (DFT) calculations to investigate the ground-state structures of $PbTiO_3$ solid solutions containing Ni, Pd, and Pt. Anomalous effective charges are reported, including the first report of negative Born effective charges for nominal +2 cations. We predict that these proposed materials will display a decreased band gap when compared to $PbTiO_3$ while maintaining or enhancing polarization. They are promising candidates for use as semiconducting ferroelectric substrates for solar conversion devices.

Introduction

Solar energy is a promising long-term solution for future energy requirements; however, current solar energy conversion devices are plagued by low efficiency.[1] Use of ferroelectric ABO_3 perovskite oxides is one approach for boosting conversion efficiency. Ferroelectric oxides possess spontaneous polarization and have been shown to produce a bulk photovoltaic effect[2] in which charged carriers, specifically electrons and holes, separate to prevent recombination. Once separated, the high-energy electrons are available for electrical work or catalytic splitting of water into hydrogen and oxygen. Currently, most solid oxide ferroelectrics have a band gap of at least 3 eV, absorbing primarily in the ultraviolet (UV) region. Since UV light comprises only 8% of the solar spectrum, new materials with a decreased band gap and large polarization would be highly desirable. One current example of a ferroelectric semiconductor is SbSI. While the band gap of SbSI is around 2 eV,[3] it is not as strongly polarized as the Pb-based ABO_3 oxides (Figure 1).

Substituting the B site of Pb-based perovskites with elements whose bonds with oxygen are less ionic and more covalent should reduce the band gap. $PbTiO_3$ is a well-known solid oxide ferroelectric which is used as an end member in a variety of solid solutions.[12,13] The desirable properties of $PbTiO_3$ have also been well studied as a model for understanding and designing other systems of technological importance.[14] In previous work, we studied the structural and catalytic properties of Pd and O-vacancy-substituted $BaCeO_3$.[15,16] In this study, we substitute the B-site of $PbTiO_3$ with group 10 metals Ni, Pd, and Pt (M), stabilized by an accompanying O vacancy. We predict that the new $PbTiO_3$-derived perovskites display significantly lower band gaps while maintaining or even enhancing the polarization of the parent $PbTiO_3$ material.

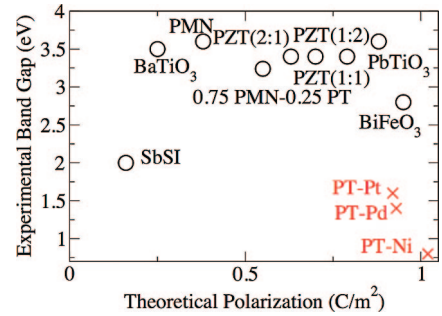

Figure 1. (○) Experimentally measured band gap[4−8] of ferroelectrics versus their theoretical polarization.[9−12] Most solid oxides have a band gap above 3 eV, except the multiferroic $BiFeO_3$. The only ferroelectrics with a band gap around 2 eV are SbSI and related compounds,[3] which are not as strongly ferroelectric as the ABO_3 oxides. (×) Estimated values for the materials proposed in this study (note high P and low E_{gap}).

Methodology

In this study, an in-house solid-state DFT code, BH, employed in previous studies[17,18] is used to relax ionic positions. Lattice

(1) Lu, D.; Takata, T.; Saito, N.; Inoue, Y.; Domen, K. *Nature* **2006**, *440*, 295.
(2) Inoue, Y.; Sato, K.; Sato, K.; Miyama, H. *J. Phys. Chem.* **1986**, *90*, 2809–10.
(3) Fong, C. Y.; Petroff, Y.; Kohn, S.; Shen, Y. R. *Solid State Commun.* **1974**, *14*, 681–5.
(4) Joshi, P. C.; Desu, S. B. *Thin Solid Films* **1997**, *300*, 289–94.
(5) Bao, D.; Yao, X.; Shinozaki, K.; Mizutani, N. *J. Phys. D: Appl. Phys.* **2003**, *36*, 2141–5.
(6) Pandeya, S.; Jamesa, A.; Ramana, R.; Chatterjeea, S.; Goyala, A.; Prakasha, C.; Goelb, T. *Physica B* **2005**, *369*, 135–42.
(7) Chan, K. Y.; Tsang, W. S.; Mak, C. L.; Wong, K. H. *Phys. Rev B* **2004**, *69*, 144111−1−5.
(8) Wan, X.; Chan, H. L. W.; Choy, C. L.; Zhao, X.; Luo, H. *J. Appl. Phys.* **2004**, *96*, 1387–91.
(9) Spanier, J. E.; Kolpak, A. M.; Urban, J. J.; Grinberg, I.; Ouyang, L.; Yun, W. S.; Rappe, A. M.; Park, H. *Nano Lett.* **2006**, *6*, 735–9.
(10) Baettig, P.; Ederer, C.; Spaldin, N. A. *Phys. Rev. B* **2005**, *72*, 214105–1–8.
(11) Grinberg, I.; Rappe, A. M. *Phase Trans.* **2007**, *80*, 351–68.
(12) Grinberg, I.; Rappe, A. M. *Phys. Rev. B* **2004**, *70*, 220101–1–4.
(13) Juhas, P.; Grinberg, I.; Rappe, A. M.; Dmowski, W.; Egami, T.; Davies, P. K. *Phys. Rev. B* **2004**, *69*, 214101–1–13.
(14) Park, S.-E.; Shrout, T. R. *J. Appl. Phys.* **1997**, *82*, 1804–11.
(15) Li, J.; Singh, U. G.; Bennett, J. W.; Page, K.; Weaver, J.; Zhang, J.-P.; Proffen, T.; Rappe, A. M.; Scott, S.; Seshadri, R. *Chem. Mater.* **2007**, 1418–23.
(16) Singh, U. G.; Li, J.; Bennett, J. W.; Rappe, A. M.; Seshadri, R.; Scott, S. L. *J. Catal.* **2007**, *249*, 347–56.
(17) Mason, S. E.; Grinberg, I.; Rappe, A. M. *Phys. Rev. B* **2004**, *69*, 161401(R)−1−4.

Table 1. Comparison of Experimental[34] and Theoretical Lattice Parameters of $PbTiO_3$ (Å) as well as Polarization[11] (C/m^2) and Band Gap (E_{gap}, eV)[5] and M-Substituted PT Solid Solution Results from This Study

	lit.	present	PT−Ni	PT−Pd	PT−Pt
a	3.91	3.86	3.77	3.80	3.83
c	4.15	4.07	12.82	12.78	12.82
c/a	1.063	1.055	3.40	3.36	3.35
P	0.88	0.93	1.02	0.93	0.92
E_{gap}	3.6	2.4	0.8	1.4	1.6

constants are optimized using the ABINIT software package.[19] The local density approximation (LDA) of the exchange correlation functional and a 4 × 4 × 4 Monkhorst-Pack sampling of the Brillouin zone[20] are used for all calculations except for the response function and Berry phase polarization[21] calculations for which a 6 × 6 × 6 grid was required to achieve convergence. The generalized gradient approximation of the exchange correlation functional was not used for this study as it overestimates the relaxed volume of the unit cell, increasing the *c/a* ratio by up to 260%.[22] All atoms are represented by norm-conserving optimized[23] designed nonlocal[24] pseudopotentials. All pseudopotentials are generated with the OPIUM code.[25] The calculations are performed with a plane wave cutoff of 50 Ry. Calculations for M (where M = Ni, Pd, and Pt) substituted $PbTiO_3$ were performed on a 1 × 1 × 3 14-atom supercell arrangement. In this arrangement one Ti in three is replaced by a group 10 metal, M, and stabilized by an O vacancy to yield $PbTi_{2/3}M_{1/3}O_{8/3}$. Such layered structures could potentially be synthesized in a thin film form by atomic layer deposition (ALD) growth.[26,27] Recently published work on $PbTi_{1/2}Fe_{1/2}O_{3-\delta}$ perovskite[28] indicates that even for high B-site substitution levels such as those studied here off-valence substituted $PbTiO_3$ can remain in the perovskite phase.

Structural DFT results for $PbTiO_3$, as shown in Table 1, agree well with experimental data. Elongation of the *c* axis to 4.07 Å is a result of the 0.45 Å relative displacement made in that direction by Pb. Ti displaces 0.32 Å as well in the same direction. This creates a polarization of 0.93 C/m^2 along *c*, close to the accepted DFT-LDA value. As expected, DFT-LDA calculations underestimate the band gap of $PbTiO_3$ by about 1 eV, in line with the well-known trend of DFT underestimation of band gaps.[29−32] Although LDA underestimates the band gap magnitudes, DFT-LDA calculations have been shown to be reliable in reproducing trends in the band gap as the material composition is changed.[33]

Results

Comparison of the relaxed structures of the three M-substituted compositions and the parent $PbTiO_3$ shows that Ni, Pd, and Pt have similar effects on the structural and electronic properties of $PbTiO_3$; however, the magnitude of these effects depends strongly on the identity of the M substituent. Replacement of the Ti−O pair with M and O vacancy leads to considerable changes in the B-site local structure and geometry. We find that all three M adopt a square-planar configuration, consistent with their +2 formal ionic charge.

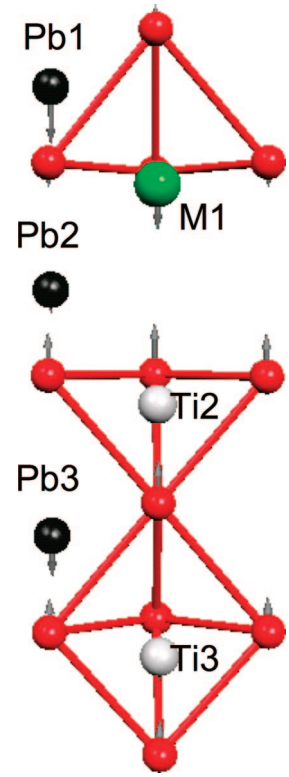

Figure 2. Structure of $Pb(Ti_{2/3}Pt_{1/3})O_{8/3}$. Black atoms are Pb, green are M (Pt is shown here), white are Ti, and red are O. Arrows are shown to indicate relative displacement from the parent tetragonal $PbTiO_3$ structure.

This configuration is stabilized by the oxygen vacancy. The vacancy−M pair is aligned with the long axis of the tetragonal unit cell, normal to the square-planar M bonding geometry. Each M has four oxygen nearest neighbors with the fifth oxygen further away. The O_6 octahedron is transformed into an $M-O_4$ complex with the fifth apical oxygen displacing away from the M. We find that the M atom moves out of the O_4 plane; Ni displaces the least and Pt the most. The displacement is toward the O vacancy and away from the remaining apical O.

Introduction of the O vacancy gives rise to significant distortions of the oxygen lattice. This increases all cation displacements, allowing larger polarization for all three M-substituted materials compared to the parent $PbTiO_3$. The four planar O atoms of the Ti atom next to the vacancy (Ti2) displace toward the vacancy, as shown in Figure 2. Due to the loss of its top apical O atom, the Ti2 atom moves farther into its cage to create a short, strong bond with the bottom apical oxygen. This results in a considerable increase in the Ti2 displacement from the center of its four planar oxygens compared to the Ti displacement in PT. Pd- and Pt-substituted PT display Ti2 off-center distortions of 0.48 and 0.51 Å, compared to 0.32 Å observed in pure PT. For Ni-doped PT the enhancement is even larger, with Ti2 distortion of 0.68 Å.

The Ti atom which retains a complete O_6 cage (Ti3) is also affected by introduction of the vacancy. Due to periodic

(18) Bennett, J. W.; Grinberg, I.; Rappe, A. M. *Phys. Rev. B* **2006**, *73*, 180102(R)−1−4.
(19) Gonze, X.; et al. *Comput. Mater. Sci.* **2002**, *25*, 478–92.
(20) Monkhorst, H. J.; Pack, J. D. *Phys. Rev. B* **1976**, *13*, 5188–5192.
(21) Resta, R. *Rev. Mod. Phys.* **1994**, *66*, 899–915.
(22) Wu, Z.; Cohen, R. E.; Singh, D. J. *Phys. Rev. B* **2004**, *70*, 104112−1−7.
(23) Rappe, A. M.; Rabe, K. M.; Kaxiras, E.; Joannopoulos, J. D. *Phys. Rev. B Rapid Commun.* **1990**, *41*, 1227–30.
(24) Ramer, N. J.; Rappe, A. M. *Phys. Rev. B* **1999**, *59*, 12471–8.
(25) http://opium.sourceforge.net.
(26) Aaltonen, T.; Ritala, M.; Sajavaara, T.; Keinonen, J.; Leskela, M. *Chem. Mater.* **2003**, *15*, 1924–28.
(27) Harjuoja, J.; Kosola, A.; Putkonen, M.; Niinisto, L. *Thin Solid Films* **2006**, *496*, 346–52.
(28) Palkar, V.; Malik, S. *Solid State Commun.* **2005**, *134*, 783–6.
(29) Sham, L. J.; Schlüter, M. *Phys. Rev. Lett.* **1983**, *51*, 1888–91.
(30) Sham, L. J.; Schlüter, M. *Phys. Rev. Lett.* **1985**, *32*, 3883–9.
(31) Hybertsen, M. S.; Louie, S. G. *Phys. Rev. Lett.* **1985**, *55*, 1418–1421.
(32) Hybertsen, M. S.; Louie, S. G. *Phys. Rev. B* **1986**, *34*, 5390–5413.
(33) van de Walle, C. G.; Martin, R. *Phys. Rev. B* **1986**, *34*, 5621–34.
(34) Shirane, G.; Pepinsky, R.; Frazer, B. C. *Acta Crystallogr.* **1956**, *9*, 131–40.

Table 2. Displacements (Å) of All Cations from O-Cage Centers for M-Substituted $PbTiO_3$

M	unit cell 1	Δz 1	unit cell 2	Δz 2	unit cell 3	Δz 3
Ni	Pb1	0.69	Pb2	0	Pb3	0.63
	Ni	0.34	Ti2	0.68	Ti3	0.52
Pd	Pb1	0.80	Pb2	0.10	Pb3	0.63
	Pd	0.38	Ti2	0.51	Ti3	0.48
Pt	Pb1	0.81	Pb2	0.16	Pb3	0.71
	Pt	0.46	Ti2	0.48	Ti3	0.46
none	Pb1	0.45	Pb2	0.45	Pb3	0.45
	Ti1	0.32	Ti2	0.32	Ti3	0.32

boundary conditions the bottom apical oxygen for Ti3 is the top apical oxygen of the next M cage. Each M prefers a square-planar coordination; so the bottom apical oxygen of Ti3 moves up. This strengthens the bond between Ti3 and its bottom apical oxygen. Due to oxygen−oxygen repulsion, the planar oxygen atom neighbors of Ti3 are forced to move up as well. Together these two effects lead to an enhancement of the Ti3 displacement from its cage center. Here too, the off-center displacement of Ti3 is largest for Ni-substituted PT (0.52 Å) and smallest for Pt-doped PT (0.46 Å), as shown in Table 2.

Our calculations show that the presence of the vacancy enhances Pb displacements except for the Pb in the plane of the vacancy. For all three M-containing structures the Pb displacement magnitudes are largest for Pb1, smaller for Pb3, and smallest for Pb2. This trend can be easily understood by considering the interplay between the changes to the oxygen lattice induced by the vacancy and the well-known requirement for creation of short, ∼2.5 Å, Pb−O bonds in perovskites.[35,36] For Pb2, a large displacement is not necessary to create the short Pb−O bonds as the O atoms in the plane below Pb2 move up into the vacancy, shortening the Pb−O distances (Figure 2). The Pb displacement from the center of the O cage (O_8 in the case of Pb2) is further diminished by the *downward* motion into the vacancy by the O atoms in the plane above Pb2. For Pb1, the distortions of the O atoms above the Pb2 into the vacancy require a large Pb1 displacement from the center of the O cage to create the short Pb−O bonds. The Pb1 displacement is also enhanced by movement of the apical oxygen of the M−O_5 cage away from the square-planar coordinated M and therefore also away from Pb1. In the case of Pb3, the coupling to Pb1 displacement and upward movement of the O atoms above Pb3 tend to enhance Pb3 displacement, but the downward movement of the O atoms below Pb3 tends to suppress it. Therefore, Pb3 displacement is smaller than that of Pb1.

We find that the Pb atom displacements increase with the ionic size of M (Table 2). For example, for Pb1 the computed ionic displacements are 0.65, 0.80, and 0.81 Å for Ni-, Pd-, and Pt-substituted PT, respectively. This is due to the larger displacements of the apical oxygen of the M−O_5 cages for the larger Pd and Pt atoms, which has a significant impact on the magnitude of the Pb displacements, as explained above. Expansion of the tetragonal *c* axis promotes ferroelectricity, allowing greater Pb ion displacements for the larger M substituents. Additionally, elongation of the *a* axis is proportional to the ionic size of M itself.

The above discussion considered apical vacancies with the M-vacancy direction parallel to the polarization $\vec{P}$. When the O vacancy is not apical, but equatorial, polarization along *c* decreases to 0.8 C/m^2 as polarization along *a* increases slightly to about 0.1 C/m^2 in all three M-substituted compositions. This occurs because both of the apical O atoms move toward M while the equatorial O, opposite the vacancy, moves away. This reorganization of O around M forces Pb to displace along *c* and *a*, resulting in a MO_4 complex in the *yz* plane and not the *xy* plane. The structures with apical vacancies are more stable, by 0.3 eV on average; however, the position of the vacancy does not change the value of the band gap. The observation that an equatorial O vacancy is higher in energy than an axial one has been observed in previous studies,[37,38] though neither discuss the effect of O vacancies on band gap.

Table 3. Nonzero Born Effective Charge Tensor Elements of All B Sites for M-Substituted PT[a]

M	Z^*_{xx}	Z^*_{yy}	Z^*_{zz}	Z^*_{xx}	Z^*_{yy}	Z^*_{zz}	Z^*_{xx}	Z^*_{yy}	Z^*_{zz}
Ni	1.0	1.0	0.03	5.6	5.6	4.8	5.6	5.6	5.5
Pd	0.75	0.75	−0.19	5.2	5.3	4.7	5.5	5.5	5.3
Pt	0.95	0.95	−0.48	5.4	5.4	4.7	5.5	5.4	5.5

[a] Shown first are the values for M, then Ti2, and finally Ti3.

Introduction of M changes the metal−oxygen bonding, leading to changes in the Born effective charges of the ions. In high-symmetry $PbTiO_3$ the calculated diagonal Z^* values are 3.7 and 6.3 for Pb and Ti ions, respectively. Due to ionic displacements these values change to 3.6 and 5.5 in the relaxed tetragonal structure for Pb and Ti ions, respectively. In M-substituted $PbTiO_3$, Pb ion Born effective charges display only minor changes from their $PbTiO_3$ values, a decrease from 3.6 to 3.5. The impact of M substitution on the Born effective charges of the B site is more significant. Z^* of the Ti atom adjacent to the vacancy is 4.8, smaller than the 5.5 in the pure PT. The Ti atom with a full O_6 shell of nearest neighbors has a Z^* of 5.5, essentially identical to the Z^* value found in tetragonal $PbTiO_3$. Surprisingly, we find that the M substitutions exhibit very small positive (Ni) or negative values of Z^*_{zz}. To our knowledge this is the first observation of negative Born effective charges for a cation. The Z^*_{zz} value decreases as the ionic size of *M* increases, reaching −0.5 for Pt, as shown in Table 3.

Negative Z^* values for nominal cations could be due to the following mechanism. The d8 M strongly favors a square-planar environment. However, the constraint of the perovskite lattice does not allow the M−O complex to be perfectly square planar as one of the apical oxygen atoms is still present. Although the distance between M and the remaining apical oxygen is quite large (2.64 Å for Ni-substituted PT), it is not large enough to make the apical oxygen insensitive to the presence of the M. For example, bond valence analysis[39] shows that the bond order for the M−apical oxygen distance is 0.174. The preference of M for a square coordination means that a build up of electron density between the apical oxygen and M is unfavorable. This build up becomes more unfavorable as M moves closer to the apical oxygen. In such a case, the apical oxygen electrons will flow away from the M. This flow of negative charge will counterbalance and then overcome the flow of positive charge due to the motion of the M cation, leading to a overall negative Z^*_{zz} for *M*.

(35) Cohen, R. E. *Nature* **1992**, *358*, 136–138.
(36) Egami, T.; Dmowski, W.; Akbas, M.; Davies, P. K. Local Structure and Polarization in Pb-Containing Ferroelectric Oxides First-Principles Calculations for Ferroelectrics. Fifth Williamsburg Workshop, Melville, New York, 1998; pp 1−10.
(37) Zhang, Z.; Wu, P.; Lu, L.; Shu, C. *Appl. Rev. Lett.* **2006**, *88*, 142902−1−3.
(38) Zhang, Z.; Wu, P.; Lu, L.; Shu, C. *J. Alloys Compd.* **2008**, *449*, 362–5.
(39) Brown, I. D. *The Bond-Valence Method Structure and Bonding in Crystals II*;: New York, 1981; pp 1−30.

We find that all three compositions exhibit polarization greater than or equal to that of the parent $PbTiO_3$ material. Polarization in a ferroelectric solid solution can be modeled as the sum of the cationic displacements multiplied by the cation Z^*.[40] Thus, at first glance the enhanced polarization of PT−Ni (for example) is surprising due to a significant decrease in Z^* of the B site due to substitution of Ti ($Z^* = 5.6$) by Ni ($Z^* = 0.03$) as well as a decreased Pb displacement for the Pb2 site. However, these effects are counterbalanced by the enhanced Pb displacement at the Pb1 and Pb3 sites and the large displacements made by the remaining O_5 and O_6 cages surrounding Ti, which induce a larger Ti−O dipole than in pure PT.

For example, in pure PT the approximate $\vec{P}$ contributions for Pb and Ti are 0.43 and 0.46 C/m^2, respectively. This is calculated as $(\Delta z_{Pb} \times Z^*_{zz})/(V)$ and $(\Delta z_{Ti} \times Z^*_{zz})/(V)$. For PT−Ni, the total Pb contribution decreases slightly to 0.41 as Pb2 does not move while Pb1 and Pb3 displace farther than in PT while maintaining their Z^*_{zz}. The increase in $\vec{P}$ of PT−Ni comes from the increased polarization of the two Ti B sites, which contribute 0.54 C/m^2, more than the Ti in pure PT. This is due to the very large enhancement of the Ti displacements in PT−Ni, as explained above. The large Ti contribution more than compensates for the lack of polarization on the Ni site ($Z^*_{zz} = 0.03$). For the PT−Pd and PT−Pt structures, the B-site-based $\vec{P}$ contribution is smaller than for PT−Ni and PT as Ti2 and Ti3 displacements are smaller and Z^*_{zz} for Pd and Pt are negative. However, the total polarization is maintained relative to PT for these two alloys because the displacements of Pb increase, enhancing the Pb contribution to $\vec{P}$.

Comparison of the three compositions shows that polarization decreases with the increased ionic size, e.g., $P = 0.92$ C/m^2 for PT−Pt and $P = 1.02$ C/m^2 for PT−Ni. This is due to the decreased displacements of Ti3 site for PT−Pt as well as the more negative Born effective charge for the PT−Pt composition.

Analysis of the electronic densities of states (DOS) shows that relative to the parent $PbTiO_3$ the band gap of the material is considerably reduced by the presence of M, reaching 0.8 eV for PT−Ni. The decrease in band gap is due to new states in the electronic structure of both the highest occupied molecular orbital (HOMO) and lowest unoccupied molecular orbital (LUMO) associated with the presence of M. In $PbTiO_3$ the HOMO is localized around O, its 2p orbitals interacting slightly with the 3d of Ti and the 6s state of Pb. The LUMO is localized around Ti and resembles 3d states. When the M and O vacancy replace Ti, the M d states fall in the $PbTiO_3$ band gap, reducing the band gap of the alloy. The HOMO is localized on M and is d_{z^2} for all three compositions. This is the highest filled d orbital for a d8 M in a square-planar configuration. The LUMO is also localized around M d states. These M d states are lower in energy than the Ti 3d, lowering the conduction band edge relative to PT. The trend in band gap may be related to the relative diffuseness of the d states of the M substituents since 3d is smaller than both 4d and 5d which are about the same size.

With the decreased band gap all three of these materials are now better suited to absorb visible light than $PbTiO_3$. This could potentially increase the solar efficiency of the next generation of solid oxide components in solar photovoltaics and hydrogen production devices.[2] Current light harvesting theories are pointing toward M-substituted solid oxide or sulfide solutions as a way to engineer a smaller band gap;[1,41,42] however, none maintain the electric polarization of the pure solid as well as those presented in this article.

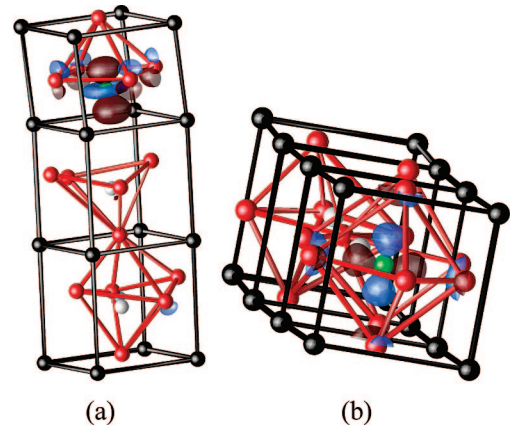

Figure 3. Pt d orbitals around the Fermi level for $PbTi_{2/3}Pt_{1/3}O_{8/3}$. Black atoms are Pb, red are O, gray are Ti, and green are Pt. (a) The HOMO is mainly d_{z^2}. (b) The LUMO is a Pt $d_{x^2-y^2}$ orbital. The relative energies of these orbitals are in line with crystal field theory for a square-planar Pt complex of C_{4v} symmetry.

Interestingly, comparison of computed band gaps and polarizations shows that the family of materials studied here does not follow the usual trend of higher polarization leading to a larger band gap. Instead, it is the oxide with the highest polarization that displays the smallest band gap. This makes the strategy pursued here a promising approach for synthesizing highly polarized semiconductor ferroelectrics.

Conclusion

We presented the first study of the ground-state structures of group 10 metal-substituted $PbTiO_3$, new solid-state oxide alloys that decrease the band gap while maintaining a large spontaneous polarization. These materials could be used in solar hydrogen production and photovoltaic applications because they can both absorb sunlight and separate carriers via the anomalous bulk photovoltaic effect seen in polarized materials. These combined properties could make these new materials more efficient at first trapping and then utilizing more of the solar spectrum than previous components of solar conversion devices.

Acknowledgment. This work was supported by the Department of Energy Office of Basic Energy Sciences, under grant number DE-FG02-07ER46431, and the Office of Naval Research, under grant number N00014-07-1-0409, and the Air Force Office of Scientific Research, under grant number FA9550-07-1-0397. Computational support was provided by the US DoD through the DURIP program and the HPCMO.

JA8052249

(40) Grinberg, I.; Suchomel, M. R.; Dmowski, W.; Mason, S. E.; Wu, H.; Davies, P. K.; Rappe, A. M. *Phys. Rev. Lett.* **2007**, *98*, 107601−1−4.

(41) Kudo, A.; Kato, H.; Tsuji, I. *Chem. Lett.* **2004**, *33*, 1534–9.

(42) Singh, D. J.; Rai, R. C.; Musfeldt, J. L.; Auluck, S.; Singh, N.; Khalifah, P.; McClure, S.; Mandrus, D. G. *Chem. Mater.* **2006**, *18*, 2696–2700.